Dynamics and mechanisms of recombination of electron–hole plasma and high-density excitons in CdS and CdSe

V. S. Dneprovskiĭ, V. I. Klimov, and M. G. Novikov

Moscow State University

(Submitted 31 May 1990; resubmitted 10 September 1990)
Zh. Eksp. Teor. Fiz. **99**, 843–859 (March 1991)

The spectral and kinetic characteristics of spontaneous and stimulated emission from CdS and CdSe crystals intensely excited by picosecond light pulses were investigated. Lowering of the excitation level caused the delay of the stimulated-emission pulse to decrease drastically from 30–40 ps to 0.6–1 ns, owing to the Mott transition from an electron–hole plasma to excitons. The observed increase of the exciton luminescence rise time with increase of the pump power is attributed to screening of the electron–hole interaction. A mechanism is proposed for the indirect recombination of an electron–hole plasma with simultaneous emission of an LO phonon. This mechanism explains the spectral positions and the shapes of the observed spontaneous and stimulated emission bands.

Screening of the Coulomb interaction in intense laser excitation of direct-band semiconductors gives rise to a transition (Mott transition) from a weakly ionized exciton gas to a strongly ionized electron–hole plasma (EHP).[1-3] Picosecond spectroscopy[4-9] provides promising methods of investigating EHP and dense exciton gas in direct-band semiconductors (such as CdS and CdSe). By exciting EHP with ultrashort pulses (USP) of light, it is possible not only to track the dynamics of EHP decay, but also to observe the Mott transition from EHP to excitons. Note, however, that numerous attempts to observe a Mott transition via changes in time-resolved luminscence, transmission, or reflection spectra have so far been unsuccessful, since the emission bands of EHP and of a dense exciton gas have practically the same spectral positions[6] and are strongly distorted by the amplification,[7] while the reflection and transmission structure typical of excitons is present also in the plasma state of the system.[3] Nor was it possible to observe the photocurrent jump due to the Mott transition from excitons to an EHP.[10]

Note that the mechanisms of the radiative decay of an EHP in CdS and CdSe remain unclear to this day. Even though these are direct-band semiconductors, the shapes of the emission and amplification bands of the EHP are best described for them by assuming indirect carrier recombination.[11,12] Equally unexplained is the strong long-wave shift of the EHP emission line relative to the exciton-level position, previously attributed to the large EHP binding energy,[4,13] but not understandable in light of the latest premise that an electron–hole condensate cannot be formed in direct-band semiconductors.[7,14] The role of stimulated processes that should influence strongly not only the luminescence spectra but also the rate of decay of both EHP and high-density excitons has likewise not been fully explained. This phenomenon is neglected in many papers, and the relaxation-time shortening recorded under intense pumping is associated only with the action of nonlinear decay mechanisms (for example, with Auger recombination[8]).

We report here an investigation of the spectral and kinetic characteristics of spontaneous and stimulated emission of CdS and CdSe crystals ($T = 80$ and 300 K), aimed at casting light on the main mechanisms of recombination of EHP and high-energy excitons and at studying the dynamics of the Mott transition from EHP to excitons.

EXPERIMENTAL RESULTS

We investigated CdS and CdSe crystal platelets of thickness $h = 10$–$60\ \mu$m at temperatures 80 and 300 K, under interband excitation of USP, not longer than 10 ps, of the second (CdSe) or third (CdS) harmonic of a neodymium laser. The maximum second- and third-harmonic pulse energies were 2.5 and 0.3 μJ, respectively. The pump radiation made a 45° angle with the sample surface and was focused into a spot 0.1–0.2 mm in diameter. We used for the spectral measurements an ISP-51 spectrograph (spectral resolution 1.5 nm in the blue-green region and 1 nm in the red region of the spectrum), and for the kinetic measurements an AGAT-SF fast photoelectronic recorder (FPR) (resolution to 5 psec).

The experimental geometry for simultaneous investigation of the spectral (kinetic) characteristics of both the spontaneous and stimulated emission produced by intense pumping was set up to project simultaneously on the spectrograph (FPR) slit the image of the excited volume and the image of the crystal face scattering the enhanced luminescence. The rise time of the spontaneous or stimulated luminescence was measured by additionally directing reference second-hramonic pulses reflected from the crystal to the FPR input.

The emission spectra of strongly pumped CdS at $T = 80$ K (excitation USP energy $W > 0.01\ \mu$J, corresponding to a power density $S > $ MW/cm^2) contained a predominant structureless broad Q band at 490–493 nm, approximately 30 meV wide at half-maximum (Fig. 1, solid line). An enhanced luminescence track appeared in the crystal at $W > 0.07$–$01\ \mu$J, with a spectrum (R line) located in the region of the long-wave wing of the Q band (Fig. 1, dashed line).

The luminescence spectra of strongly excited CdSe crystals (80 K) had a similar structure[15] and consisted of a broad Q band ($\lambda = 690$ nm) of spontaneous emission from the excitation region, and a relatively narrow R band ($\lambda = 702$ nm) of stimulated emission scattered by the sample face. The threshold for the induced processes was close to 0.2 μJ.

In the kinetic measurements, just as in the spectral ones, we recorded, simultaneously with the radiation pulses from the excited volume [solid lines in Fig. 2 (CdSe) and Fig. 3

 0038-5646/91/030468-09$03.00

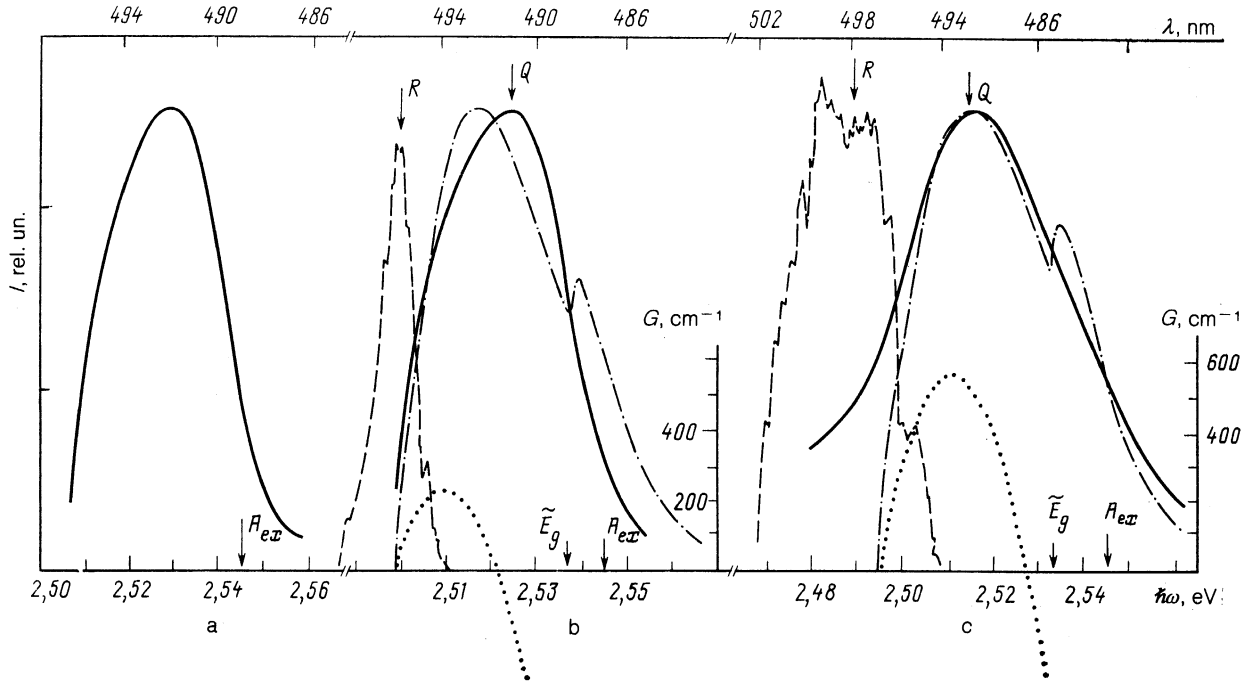

FIG. 1. CdS luminescence spectra (80 K) (solid line—radiation from excitation region, dashed—radiation scattered by sample face): $W = 0.07W_0$ (a), $0.7W_0$ (b), W_0 (c) ($W_0 = 0.3\,\mu$J). The dotted and dash-dot lines show the calculated gain and luminescence spectra (with allowance for amplification and reabsorption in the excited volume), with account taken of direct and indirect transitions (accompanied by LO-phonon emission) for the parameter values $T_e = T_{LO} = 120$ K, $l_d = 5\,\mu$m, $n_g = 0.7 \cdot 10^{18}$ (b) and 10^{18} cm^{-3} (c). The arrows mark the positions of the energy level of the A exciton and the renormalized band gap $\tilde{E}_g$ (the value of $\tilde{E}_g$ is determined by the best fit of the positions of the calculated and experimental emission spectra).

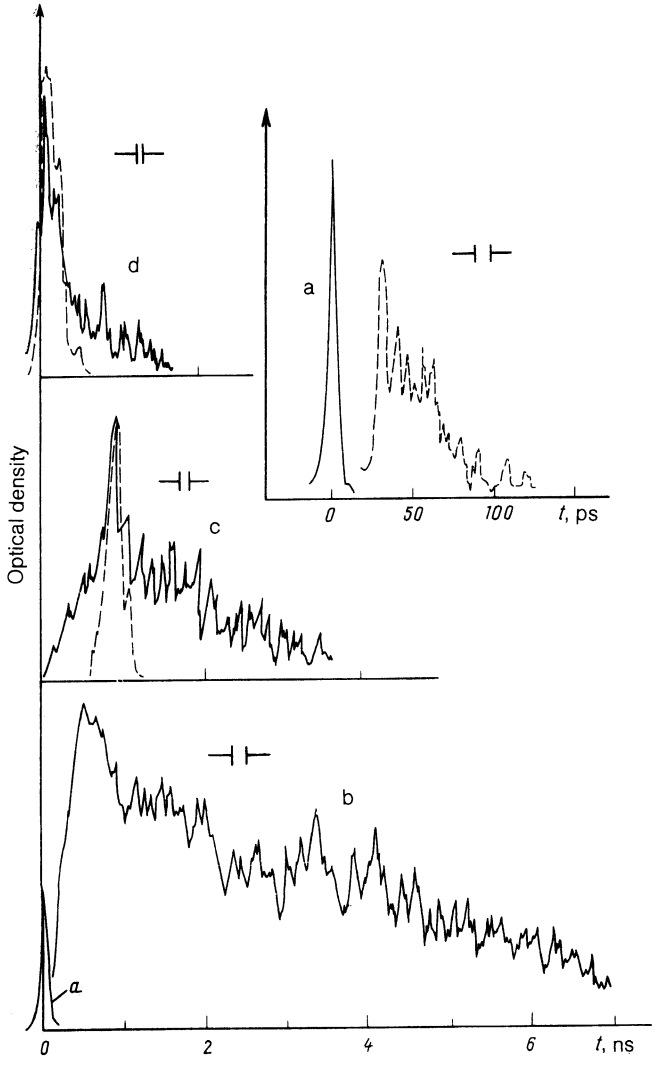

FIG. 2. Density patterns of excitation pulse (a) and of the CdSe luminescence pulses (80 K) from the excitation region (solid line) and of the radiation scattered by the sample faces (dashed line) at $W = 0.08$ (b), 0.28 (c), 0.44 (d) and 0.8 μJ (inset).

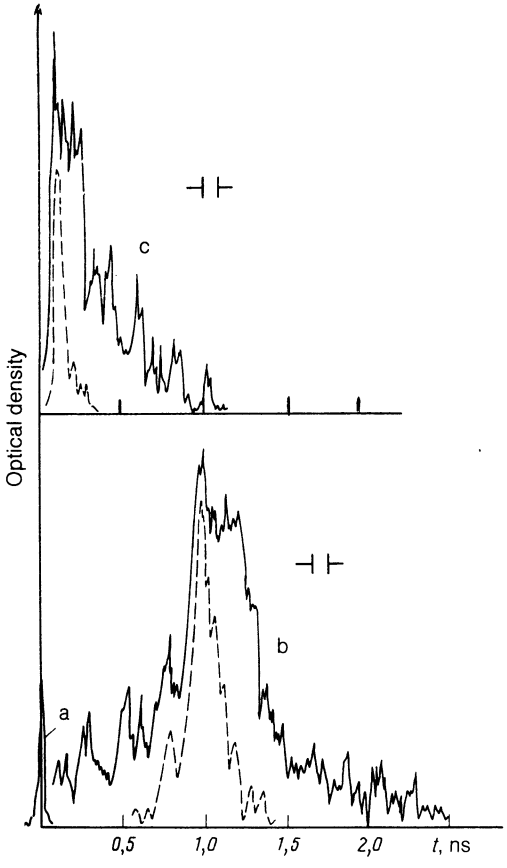

FIG. 3. Density patterns of excitation pulse (a) and of CdS luminescence pulses (80 K) from the excitation region (solid line) and of the radiation scattered by the sample face (dashed line) at $W = 0.15\,\mu$J (b) and $0.25\,\mu$J (c).

(CdS)], pulses of radiation scattered by the crystal face (dashed lines in Figs. 2 and 3). In the case of CdSe at $W = 0.08\,\mu$J, i.e., below the stimulated-radiation excitation threshold, the maximum of the luminescence pulse from the excited volume was delayed by $\Delta t = 0.6$ ns relative to the pump USP (Fig. 2b). The delay time Δt at an excitation-pulse energy $W = 0.3\,\mu$J (above the threshold of the stimulated processes) was increased to 0.9 ns (Fig. 2c). A short spike was then superimposed on the crest of the radiation pulse from the excited volume. This spike, judging from its coincidence with the amplified luminescence pulse scattered from the face of the sample and from the fast growth of the amplitude of the luminescence-pulses in the region, is due to action of stimulated effects, as attested by its coincidence with the enhanced luminescence scattered from the sample face (Fig. 2d, dashed line) and by the fast growth of the amplitude of the luminescence pulses in the region $W > 0.2$ μJ (inset, Fig. 2). Note that the onset of the stimulated emission is significantly delayed relative to the pump USP. At $W > 0.4\,\mu$J the delay of pulses from both the excitation region and scattered from the sample surface was radically shortened (Fig. 2d) and amounted at maximum pumping (close to $1\,\mu$J) to 30–40 ps (inset, Fig. 2).

A strongly shortened delay time Δt was also observed in the case of CdS (Fig. 3), from 1 ns at relatively low excitation levels to $\Delta t < 100$ ps at high USP pump energies.

Let us examine the measured characteristic luminescence-intensity relaxation times, shown for CdSe (80 K) in Fig. 4 as a plot of [1)] τ_I against I (the measured radiation relaxation characteristics of CdS crystals (80, 300 K) were reported in detail in an earlier paper[17]). At low excitation levels ($W < 0.1\,\mu$J) the luminescence pulses decreased almost exponentially (Fig. 2b) with a characteristic time τ_I close to 4 ns. Above the threshold for development of stimulated processes ($W > 0.2\,\mu$J) the relaxation of the luminescence pulse from the excitation region consisted of two sections: initial "fast" relaxation of stimulated emission and final "slow" relaxation of spontaneous emission.

The measured relaxation times τ_I differ considerably for pulses with large ($\Delta t > 0.6$ ns, region I in Fig. 4) and small ($\Delta t < 100$ ps, region II in Fig. 4) delay relative to the pump USP. The slow-relaxation time decreased with increase of the excitation level, from 4 to 1.6 ns in the former case and from 0.8 to 0.3 ns in the latter. The time of fast relaxation was 0.4–0.1 ns in the former case and increased rapidly in the latter case from 300 to 30 ps.

Figure 5 shows the results of kinetic measurements for CdSe at $T = 300$ K. No stimulated emission from the crystal

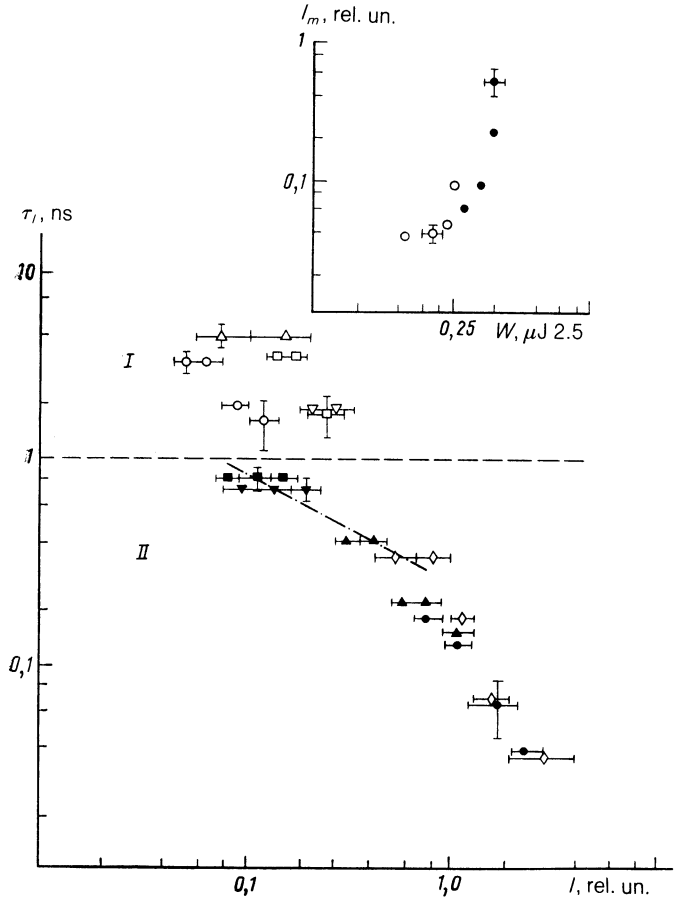

FIG. 4. Dependence of characteristic luminescence-relaxation time τ_I of CdSe (80 K) on its intensity I (the dash-dot line corresponds to $\tau_I \sim I^{-0.5}$). Region I—luminescence pulses with large delays relative to the pump USP, region II—with small delay (identical symbols are used for characteristic times determined from different sections of the decrease of one and the same luminescence pulse). The inset shows the dependence of the luminescence pulse amplitude I_m on the pumps USP energy W (○—pulses from region I, ●—from region II).

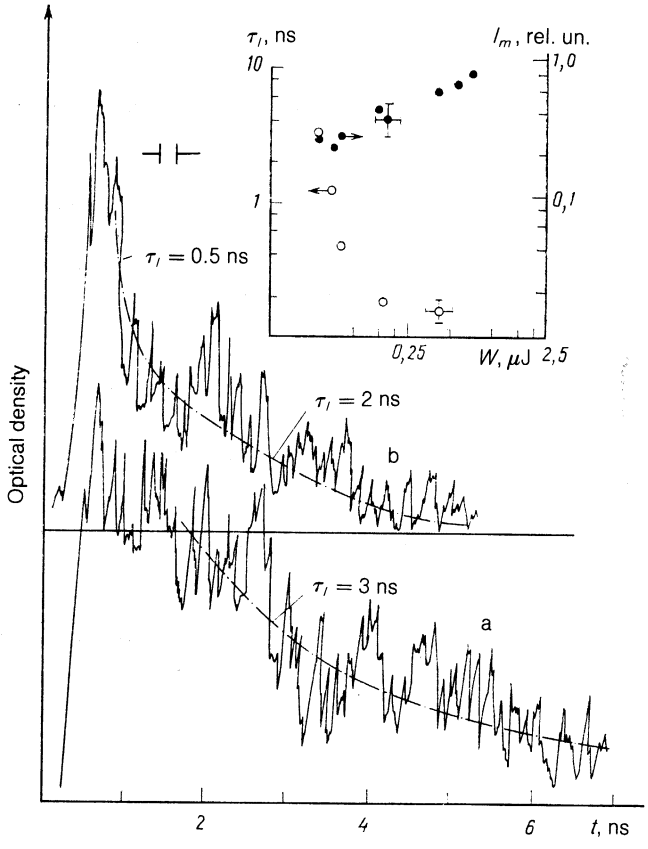

FIG. 5. CdSe luminescence pulses (300 K) at $W = 0.06$ (a) and 0.08 mJ (b). The inset shows the dependence of the luminescence pulse amplitude I_m (●) and of the characteristic relaxation time τ_I at the start of the decrease of the luminescence pulse (○) on the pump USP energy W.

face was observed in this case all the way to the maximum excitation levels. The relaxation time τ_I decreased rapidly with increase of the pump power, from 3 ns ($W = 0.06\,\mu$J) to 100–200 ps ($W = 0.8\,\mu$J). Note that the luminescence-pulse amplitude changed insignificantly in this case (inset of Fig. 5).

DISCUSSION OF RESULTS

1. Dynamics of binding of high-energy carriers into excitons

The initial density of nonequilibrium EH pairs in CdS and CdSe at the employed maximum excitation levels was close to 10^{18}–10^{19} cm^{-3} even with allowance for carrier diffusion to a depth 10–20 μm.[18] This is higher than the Mott density n_M determined from the condition[19]

$$r_D = 0{,}84 a_{ex}, \qquad (1)$$

where a_{ex} is the exciton radius, $r_D = [\varepsilon_0 kT_e/8\pi e^2 n_e]^{1/2}$ is the Debye screening radius, ε_0 is the static dielectric constant, n_e is the carrier density, and T_e is the EHP electron temperature. Using (1), we can obtain $n_M = 3\cdot 10^{17}$ cm^{-3} (CdS) and $n_M = 0.9\cdot 10^{17}$ cm^{-3} (CdSe).

Thus, at the maximum employed exitation levels, an EHP was apparently excited in the semiconductor. Related to the EHP decay are the Q band of the spontaneous emission and the R band of the stimulated emission in the spectra at $W = W_0$ (Fig. 1c). The slight changes of the luminescence spectra of CdS (Fig. 1) and CdSe (Ref. 15) as functions of the excitation level are, at first glance, evidence in favor of the existence of only one recombination mechanism (EHP decay) in the entire investigated range of the pump powers. This conclusion, however, is contradicted by the kinetic measurement results which turned out to be entirely different for high and low USP excitation energies. This difference is particularly pronoucnced in the measured delay time Δt of the stimulated-emission pulse relative to the ultrashort pump pulse: $\Delta t < 100$ ps at high excitation levels and $\Delta t = 0.6$–1 ns at low ones. This has led to the conclusion that at least two different recombination mechanisms are present: plasma recombination at high excitation levels and exciton recombination at relatively low ones.

The 30–40 ps delay corresponding to the maximum excitation levels is apparently connected with the time of EHP cooling from the initial temperature determined by the excess carrier energy 0.53 eV to the temperature at which the gain in the EHP exceeds the losses. The relatively slow cooling of EHP in polar semiconductors may be due to nonequilibrium filling of the LO-phonon modes or to screening of the electron–phonon interaction.[8,20–23] The increase of Δt at low excitation levels is apparently due to the change of the recombination mechanism and the transition from EHP to excitons. Fast diffusion broadening and expansion decrease the EHP density. At $n_e < n_M$ the delay Δt is determined by the time necessary to accumulate enough excitons for the development of stimulated processes in the exciton system.

The slowing-down of binding into excitons at near-Mott carrier densities can be attributed to screening by the EHP, as indicated by the shortening of the growth time of the luminescence intensity with decrease of the excitation level (see the experimental results in Fig. 6). In the absence of screening, the cross section σ_0 for carrier binding into excitons is independent of n_e, and the characteristic binding time $\tau_b = (\sigma_0 v_T n_e)^{-1}$ (v_T is the carrier thermal velocity) increases with decrease of the density.

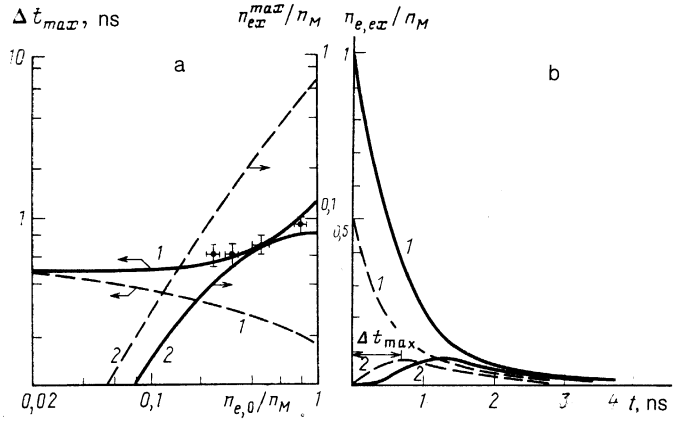

FIG. 6. a—Calculated dependence of the time Δt_{max} to reach the maximum exciton density n_{ex}^{max} (1) and of the value of n_{ex}^{max} itself (2) on the initial density $n_{e,0}$ of the photoexcited carriers without (dashed lines) and with (solid) allowance for the screening (the points show the measured exciton-luminescence buildup times). b —Calculated dependences of n_e (1) and n_{ex} (2) on t, with allowance for screening, for initial carrier densities $n_{e,0} = n_M$ (solid line) and 0.5 n_M (dashed).

Screening, on the one hand, reduces the efficacy of electron–hole interaction, and on the other lengthens the characteristic times of electron–phonon interaction. The main contribution to the energy scattering when binding into excitons takes place in CdS and CdSe at 80 K is made by polar scattering by *LO* phonons and piezoelectric scattering by acoustic phonons. In the framework of the random-phase approximation[24] the threshold carrier density needed for effective screening of electron (hole)–phonon interaction is determined from the relation[25]

$$n_c^{e,h} = \frac{\varepsilon_\infty \hbar \omega_{L0}{}^3 m_{e,h}}{24 \cdot 3^{1/2} \pi e^2 k T_e},$$

where ε_∞ is the high-frequency dielectric constant. In the case of CdSe ($T_e = 80$ K) we have $n_c^e = 1.4 \cdot 10^{17}$ cm^{-3} and $n_c^h = 8.4 \cdot 10^{17}$ cm^{-3}, which is higher than the Mott density $n_M = 1.1 \cdot 10^{17}$ cm^{-3}. The polar interaction is thus insignificantly screened during the stage of carrier binding into excitons, when $n_e < n_M$. The screening of the piezoelectric interaction can be considered in the static approximation, which yields a weak logarithmic dependence of the scattering probability on the density n_e.[26] The main cause of the slower binding of carriers into excitons is thus the screening of the electron–hole interaction. It can be taken into account in the Debye static approximation by introducing the density dependence of the dielectric constant $\varepsilon(n_e)$:[27]

$$\varepsilon(n_e) = \varepsilon_0 \left[1 - \frac{0{,}84 a_{ex}}{r_D}\right]^{-1} = \varepsilon_0 \left[1 - \left(\frac{n_e}{n_M}\right)^{1/3}\right]^{-1}, \quad (2)$$

determined in the region $n_e < n_M$, where n_M is the Mott density from Eq. (1). The cross section for carrier binding into excitons is proprtional to e^{-3} (Ref. 28) and is consequently

$$\sigma = \sigma_0 \left[1 - \left(\frac{n_e}{n_M}\right)^{1/3}\right]^3, \quad (3)$$

where σ_0 is the cross section of the process at low densities.

The binding of carriers into excitons is described by a system of two kinetic equations for the electron and exciton densities n_e and n_{ex}:

$$\frac{dn_e}{dt} = -\sigma(n_e) v_T n_e^2 + \theta n_{ex} - \frac{n_e}{\tau_e},$$
$$\frac{dn_{ex}}{dt} = \sigma(n_e) v_T n_e^2 - \theta n_{ex} - \frac{n_{ex}}{\tau_{ex}}, \quad (4)$$

under the initial conditions $n_e(0) = n_{e,0} \leqslant n_M$, and $n_{ex}(0) = 0$ (τ_e and τ_{ex} are the characteristic recombination times of the electrons and excitons, respectively). The term θn_{ex} in (4) takes into account the exciton dissociation. The value of θ was determined from the relation

$$\theta = N_T \sigma_0 v_T \exp(\varepsilon_{ex}/kT_e)$$

(ε_{ex} is the exciton binding energy,

$$N_T = \left(\frac{m_r k T_e}{2\pi\hbar^2}\right)^{3/2}, \quad m_r = \frac{m_e m_h}{m_e + m_h}$$

is the reduced mass of the electron and hole), which makes it possible to obtain in the stationary limit ($dn_e/dt = 0$, $dn_{ex}/dt = 0$, $\tau_e \to \infty$, $\tau_{ex} \to \infty$) the usual thermodynamic connection between the exciton and electron densities:

$$n_{ex} = \frac{n_e^2}{N_T} \exp\left(\frac{\varepsilon_{ex}}{kT_e}\right).$$

Calculations show that if screening is neglected ($\sigma = \sigma_0 = \text{const}$) the time Δt_{max} for reaching maximum density in the exciton subsystem increases with decrease of the initial carrier density (Fig. 6a, dashed line 1), but this does not agree with experiment. The measured times of exciton-luminescence buildup (marked by circles in Fig. 6; see also Figs. 2 and 3) decreased with decrease of the USP excitation energy, a result that could be explained by using (3) for the dependence of the cross section σ on the carrier density. The time Δt_{max} decreases then with decrease of $n_{e,0}$ (see the kinetic $n_e(t)$ and $n_{ex}(t)$ dependences in Fig. 6b). The best agreement with experiment (solid line 1 in Fig. 6a) was obtained at $\sigma_0 = 0.15 \cdot 10^{-13}$ cm^2, $\tau_e = 0.8$ ns, and $\tau_{ex} = 4$ ns (the times τ_e and τ_{ex} correspond to the measured relaxation times in the case of spontaneous recombination of EHP and excitons, respectively; see the data of Fig. 4). Figure 6a shows also the calculated dependences of the maximum exciton density n_{ex}^{max} on $n_{e,0}$, obtained with (solid line 2) and without (dashed line 2) allowance for screening. Note that the influence of screening weakens the dependence of n_{ex}^{max} on $n_{e,0}$ at initial carrier densities close to n_M.

2. Mechanisms of internal recombination of EHP

The EHP—exciton gas transition corresponds to a carrier density at which the energy position of the renormalized edge of the conduction bands coincides with the exciton level.[29] In the case of direct plasma recombination there should be located in the same spectral region (near the exciton level whose position hardly varies with the pump power[29]) lines of spontaneous and stimulated EHP emission, but this does not agree with the spectral positions of the Q and R luminescence bands (Fig. 1), which were appreciably shifted towards longer wavelengths. The strong long-wave shift of these bands can be explained by assuming that the dominant mechanism of EHP decay is indirect annihilation of the carriers with emission, in the mixed plasmon-phonon mode[30], of a quantum $\hbar\omega_+$ having an energy higher than or close to the *LO*-phonon energy $\hbar\omega_{LO}$. The role of such processes is particularly important in the case of a nondegenerate EHP whose emission, corresponding to direct transitions, is strongly reabsorbed in the exciting volume as a result of the appreciable excess of the EHP diffusion length over the effective reabsorption length.

In the considered energy region $n_e \sim n_M \sim 10^{17}$ cm^{-3} the plasmon energy $\hbar\omega_p$ is considerably less than $\hbar\omega_{LO}$, so that one can neglect plasmon–phonon mixing and consider an EHP recombination process accompanied by emission of an *LO* phonon. The form of the plasma emission band for this process $I_i(\hbar\omega)$ was calculated using relation (A3) (see the Appendix). The EHP luminescence spectrum in direct interband recombination was determined using the equation

$$I_d(\hbar\omega) = \frac{2\pi}{\hbar} |H_{c,v}^{ev}|^2 f_e\left(\frac{\hbar\omega - \tilde{E}_g}{1 + 1/\beta}\right) f_h\left(\frac{\hbar\omega - \tilde{E}_g}{1+\beta}\right) g_c(\hbar\omega - \tilde{E}_g), \quad (5)$$

where $\tilde{E}_g$ is the renormalized band gap, f_e and f_h are the carrier energy distribution functions, $\beta = m_h/m_e$, and

$|H_{c,v}^{ev}|$ is the matrtix element of the interband photon transition [see (A2)], and

$$g_e(\hbar\omega-\bar{E}_g)=\frac{2^{1/2}m_r^{3/2}}{\pi^2\hbar^3}(\hbar\omega-\bar{E}_g)^{1/2}$$

is the combined density of states. The total EHP emission spectrum $I(\hbar\omega)$ was calculated by summing the spectra $I_d(\hbar\omega)$ and $I_i(\hbar\omega)$.

We calculated the gain spectra for the direct ($G_d(\omega)$) and indirect ($G_i(\hbar\omega)$) transitions:

$$G_d(\hbar\omega)=\frac{n}{c}I_d(\hbar\omega)\left[1-\exp\left(\frac{\hbar\omega-\bar{E}_g-\mu_e-\mu_h}{kT_e}\right)\right], \quad (6)$$

$$G_i(\hbar\omega)=\frac{n}{c}I_i(\hbar\omega)\left[1-N_{LO}\exp\left(\frac{\hbar\omega-\hbar_{LO}-\bar{E}_g-\mu_e-\mu_h}{kT_e}\right)\right], \quad (7)$$

where μ_e and μ_h are the chemical potentials of the electrons and holes, N_{LO} is the number of phonons in the $\hbar\omega_{LO}$ mode (T_{LO} is the phonon temperature), c is the speed of light in vacuum, and n is the refractive index of the semiconductor. A gain in direct transitions is possible only under the condition

$$\mu_e+\mu_h\geqslant 0, \quad (8)$$

which can be regarded also as a criterion for EHP transitions from a nondegenerate state into a degenerate one. A similar condition for indirect transitions ($G_i\geqslant 0$) can be obtained from (7):

$$\mu+\mu_h\geqslant -\frac{T_e}{T_{LO}}\hbar\omega_{LO}. \quad (9)$$

Note that the density threshold n_i for induced processes in indirect transitions is significantly lower than the density threshold n_d for direct ones. In the case of CdS, for example, at $T_e=T_{LO}=80$ K, we have $n_d=6.6\cdot 10^{17}$ cm^{-3} and $n_i=6.6\cdot 10^{16}$ cm^{-3}.

As already noted, a typical diffusion length of EHP in CdS and CdSe can reach $l_d>10\,\mu$m. At a gain (absorption) $|G|\geqslant 10^2$ cm^{-1} the product $|G|l_d$ approaches unity, thus pointing to the need for taking into account the influence of amplification and reabsorption processes on the line shape of the luminescence from the excited volume of the sample. The enhanced luminescence spectrum $I_{st}(\hbar\omega)$ was calculated using the relation

$$I_{st}(\hbar\omega)=I(\hbar\omega)\frac{\exp[G(\hbar\omega)l_d]-1}{G(\hbar\omega)l_d},$$

where $G(\hbar\omega)=G_d(\hbar\omega)+G_i(\hbar\omega)$.

Figure 7 shows by way of example the enhanced EHP luminescence (spontaneous and stimulated) and amplification (absorption) spectra in CdS with allowance for direct and indirect carrier recombination, at $n_e=5\cdot 10^{17}$ cm^{-3} and $T_e=T_{LO}=60$ and 120 K, and for the following semiconductor parameters: $m_e=0.185m_0$, $m_h=1.105m_0$, $\varepsilon_0=8.58$, $\varepsilon_\infty=5.26$, $\hbar\omega_{LO}=38$ meV (Ref. 31). The calculations have shown that even if reabsorption is disregarded the amplitude of the indirect recombination (I_i^{max}) is larger than the amplitude of the band corresponding to direct recombination (I_d^{max}), with the ratio of these amplitudes increasing with increase of temperature (inset of Fig. 7). Allowance for reabsorption increases the ratio I_i^{max}/I_d^{max} even more. Note that the gain for indirect transitions can become appreciable even for a nondegenerate EHP. For example, at $T=60$ K and $n_e=5\cdot 10^{17}$ cm^{-3} (Fig. 7a) the plasma is only at the threshold of degeneracy and the maximum gain in the direct recombination band is about 10 cm^{-1}, as against more than 500 cm^{-1} in the spectral region corresponding to indirect transitions.

The measured emission spectra of CdS (Fig. 1) were compared with the calculated EHP spectra. Note that in the description of the EHP emission spectra in CdS and CdSe, assuming zero-phonon recombination (see. e.g., Refs. 11 and 18), principal attention is usually paid only to a satisfactory description of the form of the recorded spectra, since it is impossible to reconcile the EHP densities that ensure the required positions of an emission line and its width. In the framework of the proposed model it is possible to describe simultaneously the emission line shape as well as its position.

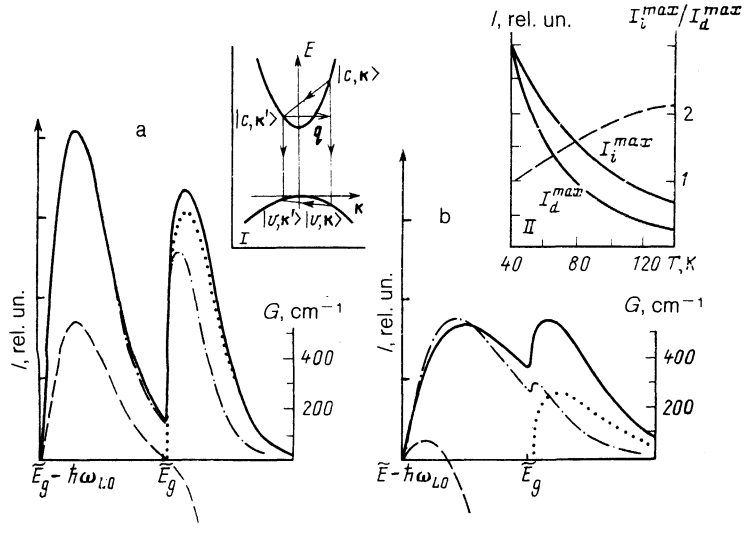

FIG. 7. Calculated EHP spectra $n_e=5\cdot 10^{17}$ cm^{-3}, $l_d=5\,\mu$m, and $T_e=T_{LO}=60$ (a) and 120 K (b): solid and dashed lines—spontaneous-luminescence and amplification lines, respectively, obtained with allowance for direct and indirect transitions, dots—spontaneous-luminescence spectrum of direct transition, dash-dot—total EHP emission spectrum with allowance for absorption and reabsorption in the excited volume. Inset I—scheme of indirect transitions in EHP for simultaneous emission of an LO phonon with wave vector $\mathbf{q}$. Inset II—calculated temperature dependences of the band amplitudes of the direct (I_d^{max}) and indirect(I_i^{max}) recombination and of their ratio (I_i^{max}/I_d^{max}).

CdS spectra corresponding to EHP recombination at 80 K were considered. The criterion for the determination of the system state were the kinetic relations, viz., 0.21 and 0.3 μJ pump USP corresponded to a small delay of the development of the stimulated-emission pulse, thus indicating that the system is in a plasma state. The best description of the form of the recorded spectra was obtained at the parameter values $T_e = T_{LO} = 120$ K, $n_1 = 0.7 \cdot 10^{18}$ cm^{-3} ($W_1 = 0.21$ μJ) and $n_2 = 10^{18}$ cm^{-3} ($W_2 = 0.3\,\mu$J), $l_d = 5\,\mu$m. To reconcile the energy positions of the calculated and experimental luminescence bands it must be recognized that at $n_e = n_M$ the renormalized edge $\tilde{E}_g$ of the bandgap has the same spectral position as the exciton level E_{ex}. An additional shift of $\tilde{E}_g$ relative to E_{ex} is produced at $n_e > n_M$ and is due to the renormalization of the band gap, defined in the static-screening approximation by the relation

$$\Delta E = |\tilde{E}_g - E_{ex}| = \varepsilon_{ex}\left[\left(\frac{n}{n_M}\right)^{1/3} - 1\right]$$

($\varepsilon_{ex} = 29$ meV for CdS, Ref. 31). At $n_M = 4.4 \cdot 10^{17}$ cm^{-3} ($T_e = 120$ K) and at the densities n_1 and n_2 used in the description of the shapes of the experimental spectra, the values of ΔE are close to 8 and 15 meV, respectively, close to the shift that ensures the best agreement of the position of the calculated band with the experimental, viz., 8 meV for spectrum *b* of Fig. 1, and 12 meV for spectrum *c*.

Note that the emission bandwidth of the stimulated luminescence scattered from the crystal faces was located in the long-wave region in which amplification is observed according to the calculated $G(\hbar\omega)$ spectra (Fig. 1). This disparity can be explained by taking into account the evolution dynamics of the stimulated and spontaneous emissions. Stimulated processes develop in EHP almost immediately after the action of the excitation USP and decrease rapidly the density of the system, in which a relatively slow spontaneous decay is subsequently observed. Thus, in the EHP stimulated-decay stage, during which the amplified-luminescence *R* band is in fact recorded, the average EHP density can be considerably higher than the average density of the plasma in its subsequent decay corresponding to the *Q* band of the emission from the excited volume.

3. Relaxation characteristics of the emission of EHP and excitons of high density

As already noted, the decreases of the luminescence pulses emitted by an excited volume at pump energies W exceeding the stimulated-emission threshold consisted of two sections: initial "fast" relaxation (stimulated emission) and final "slow" relaxation (spontaneous emission). Whereas the stimulated-luminescence intensity is an integral characteristic that depends on the prior history of the system, the spontaneous-luuminescence intensity is determined only by the instantaneous density of the recombining particles. It is therefore just the slow-decrease sections that can be used to determine the relaxation characteristics of the investigated system.

In the case of CdSe, luminescence pulses slightly delayed relative to the pump USP (EHP recombination) corresponded to slow-relaxation times in the range 0.3 = 0.8 ns. The time τ_I varied in this case with I nearly like $I^{-1/2}$ (Fig. 4), as is typical of bimolecular recombination.[17] Note, however, that one cannot exclude also a possible influence of stimulated processes, which shorten τ_I for intense pumping. This effect is particularly pronounced at a sample temperature 300 K, when an insignificant increase of the excitation intensity shortened rapidly the characteristic relaxation time (Fig. 5). The observed accompanying slight changes of the pulse luminescence pump amplitude, I_m (inset in Fig. 5) pointed to insignificant changes of the density of the recombining particles, and thus altered τ_I substantially via some nonlinear recombination mechanism [e.g., the Auger process to which the shortening of the CdSe luminescence-intensity relaxation times (300 K) are attributed in Ref. 8]. The most probable cause of the decay acceleration is in this case stimulated emission which, however, in view of peculiarities of its directivity pattern, does not contribute directly to luminescence from the excitation region.

Luminescence pulses with long delay times Δt (Fig. 2) corresponded to recombination of a dense exciton gas. The slow relaxation times amounted in this case to 1.6–4 ns. These values of τ_I are apparently the characteristic recombination times of a high-density exciton gas.

We list in conclusion the main results of our study.

1. Kinetic measurements made it possible to record a transition from EHP to a high-density exciton gas. A criterion was proposed for distinguishing the plasma and exciton states of a system by means of the delay time of a stimulated luminescence from a semiconductor excited by USP of light: long delays ($\Delta t > 0.6$–1 ns) of the development of a luminescence pulse correspond to exciton recombination, and short delays ($\Delta t < 100$ ps) correspond to EHP recombination.)

2. Electron–hole interaction was shown to influence the characteristic times of carrier binding into excitons, as manifested by an increase of the exciton-luminescence buildup with increase of the excitation level at near-Mott carrier densities.

3. A mechanism was proposed for indirect recombination of an electron–hole plasma with simultaneous emission of an *LO* phonon (photon $\hbar\omega_+$ of a mixed plasmon–phonon mode in strong plasmon–phonon mixing). This mechanism accounts for the spectral positions and the shapes of the observed spontaneous- and stimulated-emission bands.

APPENDIX

The EHP emission band shape in indirect carrier recombination accompanied by *LO*-phonon emission was calculated in second-order perturbation theory, using the relation

$$I_i(\hbar\omega) = \sum_{\mathbf{k},\mathbf{k}'} \frac{2\pi}{\hbar}\left(|H^{epv}_{c\mathbf{k},v\mathbf{k}'}|^2 + |H^{evp}_{c\mathbf{k},v\mathbf{k}'}|^2\right) f_e(\mathbf{k}) f_h(\mathbf{k}') \times \delta(E_e(\mathbf{k}) + E_h(\mathbf{k}') + \tilde{E}_g - \hbar\omega - \hbar\omega_{LO}), \quad \text{(A1)}$$

where $H^{epv}_{c\mathbf{k},v\mathbf{k}'}$ and $H^{evp}_{c\mathbf{k},v\mathbf{k}'}$ are composite matrix elements for the transition from state $|c\mathbf{k}\rangle$ of the conduction band into a state $|v\mathbf{k}'\rangle$ of the valence band via an intermediate virtual state $|c\mathbf{k}'\rangle$ in the conduction band or $|v\mathbf{k}\rangle$ in the valence band, respectively (the scheme of these transitions is shown on the inset of Fig. 7), $f_e(\mathbf{k})$ and $f_h(\mathbf{k})$ are the carrier energies reckoned from the bottoms of the corresponding bands. The composite matrix elements $H^{epv}_{c\mathbf{k},v\mathbf{k}'}$ and $H^{evp}_{c\mathbf{k},v\mathbf{k}'}$ are defined by the expressions

$$H^{epv}_{\mathbf{ck},v\mathbf{k}'}=\frac{H^{ep}_{\mathbf{ck},c\mathbf{k}'}H^{ev}_{c\mathbf{k}',v\mathbf{k}'}}{(1+\beta)E_e(\mathbf{k})-(\hbar\omega_{LO}+\beta\hbar\bar{\omega})},$$

$$H^{evp}_{\mathbf{ck},v\mathbf{k}'}=\frac{H^{ev}_{\mathbf{ck},v\mathbf{k}}H^{ep}_{v\mathbf{k},v\mathbf{k}'}}{(1+1/\beta)E_e(\mathbf{k}')-(\hbar\omega_{LO}+\hbar\bar{\omega}/\beta)},$$

where $H^{ev}_{\mathbf{ck},v\mathbf{k}}$ and $H^{ev}_{\mathbf{ck}',v\mathbf{k}'}$ are the matrix element of the interband photon transition and are assumed equal by virtue of their weak dependence on the wave vector:[32]

$$|H^{ev}_{\mathbf{ck},v\mathbf{k}}|^2=|H^{ev}_{\mathbf{ck}',v\mathbf{k}'}|^2=|H^{ev}_{c,v}|^2=2\pi e^2\hbar^2|p_x|^2/(m_0{}^2\varepsilon_\infty\hbar\omega) \tag{A2}$$

[m_0 is the free-electron mass, p_x is a momentum matrix element for the interband transition and is defined as $|p_x|^2=(m_0^2/2m_e)E_g$ (Ref. 32)], $H^{ep}_{\mathbf{ck},c\mathbf{k}'}$ ($H^{ep}_{v\mathbf{k},v\mathbf{k}'}$) is an intraband phonon-transition matrix element for polar optical scattering

$$|H^{ep}_{\mathbf{ck},c\mathbf{k}'}|^2=|H^{ep}_{v\mathbf{k},v\mathbf{k}'}|^2=|H^{ep}_{\mathbf{k},\mathbf{k}'}|^2$$

$$=\frac{1}{V}2\pi e^2\hbar\omega_{LO}\left(\frac{1}{\varepsilon_\infty}-\frac{1}{\varepsilon_0}\right)\frac{1}{q^2},$$

see Ref. 26, where $\mathbf{q}=(\mathbf{k}-\mathbf{k}')$ is the emitted-phonon wave vector and $\hbar\bar{\omega}=\hbar\omega+\hbar\omega_{LO}-\tilde{E}_g$.

An expression similar to (A1) is used to calculate the emission spectrum of an electron–hole liquid in Ge or Se (Ref. 33). For indirect-band semiconductors, however, the spectrum calculation can be substantially simplified in view of the weak dependence of the phonon-transition matrix element on the wave vectors $\mathbf{k}$ and $\mathbf{k}'$, as is the case for allowed intervalley transitions. The squared modulus of the matrix element in (A1) is then taken outside the summation sign and the resultant spectrum is determined by convolution of the distribution functions f_e and f_h (Ref. 33).

The strong dependence of the matrix element $H^{ep}_{\mathbf{k},\mathbf{k}}$ for the considered case of intraband polar scattering near the point Γ of the Brillouin zone makes it impossible to go directly from summation over $\mathbf{k}$ and $\mathbf{k}'$ to integration over the energies. The sum in (A1) was therefore calculated in two stages: the summation over $\mathbf{k}'$ was first replaced by integration over the wave vector $\mathbf{q}$ of the emitted phonon, and then the summation over $\mathbf{k}$ was reduced to integration over energy. The screening of the electron–phonon interaction was taken into account to eliminate the divergence arising in the integral over $\mathbf{q}$ at $\mathbf{q}_{\min}=0$ [$\mathbf{q}_{\min}$ is the minimum wave vector of the emitted phonon; see (A4)].

In the static-screening approximation we have $|H^{ep}_{\mathbf{k},\mathbf{k}-\mathbf{q}}|^2\sim 1/(q^2+q_D^2)$, where $q_D=1/r_D$ is the reciprocal Debye screening length. At the temperatures and densities used by us the screening is greatly weakened by dynamic effects. This was taken into account by introducing an additional parameter $\Lambda<1$, viz., $|H^{ep}_{\mathbf{k},\mathbf{k}-\mathbf{q}}|^2\propto 1/(q^2+\Lambda q_D^2)$. Note that Λ has little effect on the form and intensity of the emission line. For example, when Λ was varied from 1 to 10^{-2} the emission-line amplitude increased by less than a factor of two.

The final expression for the form of the EHP recombination band with simultaneous emission of an *LO* phonon is

$$I_i(\hbar\omega)=\frac{e^2\hbar\omega_{LO}m_em_h|H^{ev}_{c,v}|^2}{\pi^2\hbar^5}\left(\frac{1}{\varepsilon_\infty}-\frac{1}{\varepsilon_0}\right)$$

$$\times\left[\int_0^{\hbar\bar{\omega}}\frac{dE_ef_e(E_e)f_h(\hbar\bar{\omega}-E_e)}{[(1+\beta)E_e-(\hbar\omega_{LO}+\beta\hbar\bar{\omega})]^2+\Gamma^2}\ln\left(\frac{(q^c_{max})^2+\Lambda q_D{}^2}{(q^c_{min})^2+\Lambda q_D{}^2}\right)\right.$$

$$\left.+\int_0^{\hbar\bar{\omega}}\frac{dE_hf_h(E_h)f_e(\hbar\bar{\omega}-E_h)}{[(1+1/\beta)E_e-(\hbar\omega_{LO}+\hbar\bar{\omega}/\beta)]^2+\Gamma^2}\ln\left(\frac{(q^v_{max})^2+\Lambda q_D{}^2}{(q^v_{min})^2+\Lambda q_D{}^2}\right)\right], \tag{A3}$$

where

$$q^c_{max}=\frac{2^{1/2}}{\hbar}[(m_eE_e)^{1/2}+(m_h(\hbar\bar{\omega}-E_e))^{1/2}],$$

$$q^c_{min}=\frac{2^{1/2}}{\hbar}[(m_eE_e)^{1/2}-(m_h(\hbar\bar{\omega}-E_e))^{1/2}], \tag{A4}$$

$$q^v_{max}=\frac{2^{1/2}}{\hbar}[(m_hE_h)^{1/2}+(m_e(\hbar\bar{\omega}-E_h))^{1/2}],$$

$$q^v_{min}=\frac{2^{1/2}}{\hbar}[(m_hE_h)^{1/2}-(m_e(\hbar\bar{\omega}-E_h))^{1/2}].$$

Note that at a high temperature T_e the indirect transitions make a substantial contribution to the emission also in the spectral region $\hbar\omega\geqslant\tilde{E}_g$ corresponding to direct transitions. A divergence arises when $I_i(\hbar\omega)$ is calculated near $\hbar\omega=\tilde{E}_g$ and is eliminated by introducing a damping coefficient Γ^2 in the denominators of the integrands of (A2) (it was assumed in the calculations that $\Gamma=kT_e$).

[1)] Value of τ_I (instantaneous relaxation time of luminescence intensity) on different sections of the decrease of the down slope of the luminescence-pulse, determined using $\tau_I=-I(\partial I/\partial t)^{-1}$, where I is the luminescence intensity.[16]

[1] J. Shah, M. Combescot, and A. H. Dayem, Phys. Rev. Lett. **38**, 1497 (1977).
[2] G. B. Norris and K. K. Bajaj, Phys. Rev. B **26**, 6706 (1982).
[3] H. Schwizer, A. Forchel A. Hangleiter *et al.*, Phys. Rev. Lett. **51**, 698 (1983).
[4] M. Hayashi, H. H. Saito, and S. Shionya, Sol. St. Comm. **25**, 833 (1977).
[5] M. Pugnet, A. Cornet, J. Collet, and M. Brousseau, Sol. St. Comm. **36**, 85 (1980).
[6] Y. Unuma, Y. Abe, Y. Masumoto, and S. Shionya, Phys. Stat. Sol. (b) **125**, 735 (1984).
[7] H. Saito and E. O. Gobel, Phys. Rev. B **31**, 2360 (1985).
[8] M. R. Junnarkar and R. R. Alfano, *ibid.* **34**, 7045 (1986).
[9] A. A. Klochikhin, B. S. Razbiring, D. K. Nelson *et al.*, Phys. Stat. Sol (b) **147**, 727 (1988).
[10] V. D. Egorov, G. O. Müller, R. Zimmermann *et al.*, Sol. St. Comm. **38**, 271 (1981).
[11] K. Bohnert, G. Schmieder, C. Klinshirn *et al.*, Phys. Stat. Sol. (b) **98**, 175 (1980).
[12] O. Hildebrand, E. O. Goebel, K. M. Romanek *et al.*, Phys. Rev. B **17**, 4775 (1978).
[13] V. G. Lysenko, V. I. Revenko, T. G. Tratas, and V. V. Timofeev, Zh. Eksp. Teor. Fiz. **68**, 335 (1975) [Sov. Phys. JETP **41**, (1975)].
[14] S. W. Koch, Solid St. Comm. **35**, 419 (1980).
[15] V. S. Dneprovskiĭ, V. I. Klimov, and M. G. Novikov, Pis'ma Zh. Eksp. Teor. Fiz. **51**, 219 (1990) [JETP Lett. **51**, 249 (1990)].
[16] V. S. Dneprovskiĭ, V. I. Klimov, and E. D. Martynenko, Fiz. Tverd. Tela (Leningrad) **23**, 819 (1981) [Sov. Phys. Solid State **23**, 465 (1981)].
[17] V. S. Dneprovskiĭ, V. I. Klimov, and M. G. Novikov, *ibid.* **30**, 2938 (1988) [**30**, 1694 (1988)].
[18] F. A. Majumder, H. E. Swoboda, H. E. Kempf and C. Klinsirn, Phys. Rev. B **32**, 2407 (1985).

[19] N. F. Mott, *Metal–Insulator Transitions*, Barnes & Noble, 1974.
[20] J. Shah, A. Pimczur, A. C. Gossard, and W. Wiegmann, Physica B **134**, 174 (1985).
[21] K. Kash and J. Shah, *ibid.* **134**, 189 (1985).
[22] R. Maltrameyunas, A. Zhukauskas, and G. Tamulaïtis, Zh. Eksp. Teor. Fiz. **91**, 1909 (1986) [Sov. Phys. JETP **64**, 1132 (1986).
[23] P. Kocevar, Physica B **134**, 155 (1985).
[24] D. Pines, *Elementary Excitations in Solids*, Benjamin 1963, Sec. 3.5.
[25] E. J. Yoffa, Phys. Rev. B **23**, 1909 (1981).
[26] V. F. Gantmakher and N. B. Levinson, *Carrier Scattering in Metals and Semiconductors* [in Russian], Nauka, 1984, p. 79.
[27] W. Ebeling, W. Kraeft, and D. Kremp, *Theory of Bound States and Ionization Equilibrium in Plasmas and Solids*, Akademie Verlag, Berlin, 1976.
[28] V. N. Abakumov V. I. Perel', and I. N. Yasievich, Zh. Eksp. Teor. Fiz. **78**, 1240 (1980) [Sov. Phys. JETP **51**, 626 (1980)].
[29] R. Zimmermann, Phys. Stat. Sol. (b) **146**, 371 (1988).
[30] J. F. Muller and H. Haug, J. Lumin. **37**, 97 (1987).
[31] B. Segal and M. Marple, in *Physics and Chemistry of II-VI Compounds* [Russ. Transl., S. A. Medvedev, ed.), Mir (1970), p. 246.
[32] B. Ridley, *Quantum Processes in Semiconductors*, Mir, M., 1986.
[33] T. Rice, J. Hansel, T. Fillips, and G. Thomas, *Electron–Hole Liquids in Semiconductors* [Russ. Transl.] Parts I and IV Sec. 8, Mir, M., 1980.

Translated by J. G. Adashko